Status of the measurements of Higgs boson properties with the ATLAS detector

Bruce Mellado[1]

School of Physics, University of the Witwatersrand, Johannesburg 2050, South Africa

Abstract. The observation of a new particle consistent with a Higgs boson by the ATLAS and CMS experiments at the Large Hadron Collider (LHC) is now well established. With the approaching of the Run II data taking the analysis of Run I data is coming to a close. Measurements of Higgs boson properties with the ATLAS detector using Run I data are reviewed. This includes the measurement of the mass, compatibility of couplings and Spin/CP quantum numbers with the Standard Model, and the measurement of differential cross-sections. Long-term prospects of these measurements with the High-Luminosity LHC are also discussed. Prospects for Run II data taking are inferred.

1. Introduction

With the discovery of a new boson consistent with that predicted in the Standard Model (SM) by the ATLAS [1] and CMS [2] collaborations at the Large Hadron Collider (LHC), significant efforts have been made in the exploration of its properties. Here the status of these measurements is summarized, with emphasis on the results published by the ATLAS collaboration. Overall, both experiments display a consistent picture with regards to the newly discovered boson.

The exploration of the Higgs boson has branched out into a different set of relevant aspects. These include the measurements of the mass, spin/CP quantum numbers,[2] production cross-sections, and its overall compatibility with the SM. Not just for purposes of presentation, it is important to establish an order in which the results are presented. It is convenient put in place a logical succession of measurements consistent with the evolution from the most basic to the most complex. This ordering does not necessarily coincide with the order in which results are reported by the experiments.

In this light, the paper is organized as follows: Sections 2 and 3 summarize recent results of the mass and spin/CP quantum number measurements; Section 4 summarizes recent results of the total and differential cross-sections. Section 5 sums up measurements of the signal strenghts with respect to the SM. Section 6 gives a brief overview of future prospects, followed by Section 7, with summary and conclusions.

2. Mass measurement

The mass of a particle is its most basic property. The Higgs boson mass is a fundamental parameter of nature. The ATLAS and CMS collaborations have recently combined

[1] E-mail: Bruce.Mellado@wits.ac.za

[2] C stands for charge conjugation and P for parity, or space inversion.

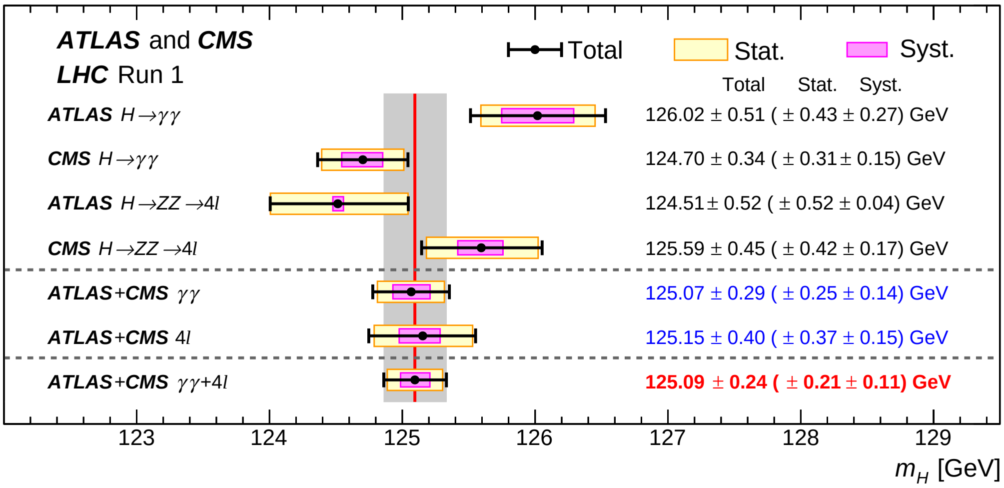

Figure 1. Summary of Higgs boson mass measurements from the individual analyses of ATLAS and CMS and from the combined analysis presented in Ref. [3]. The systematic (narrower, magenta-shaded bands), statistical (wider, yellow-shaded bands), and total (black error bars) uncertainties are indicated. The (red) vertical line and corresponding (gray) shaded column indicate the central value and the total uncertainty of the combined measurement, respectively.

measurements of the Higgs boson mass, m_H, using the most sensitive decay channels: the di-photon and $H \to ZZ^* \to 4\ell, \ell = e, \mu$ decays. With both these decays the experiments can reconstruct m_H with excellent resolution. The measurements with the di-photon and $H \to ZZ^* \to 4\ell$ channels are complementary in that the former displays the largest number of Higgs boson decay, where the latter exhibits an excellent signal-to-background ratio greater than one.

Figure 1 displays the results of the mass measurements using the two channels independently, their combination and the total combination. Results are obtained with integrated luminosities of approximately $5\,\mathrm{fb}^{-1}$ at $\sqrt{s} = 7\,\mathrm{TeV}$ and $20\,\mathrm{fb}^{-1}$ at $\sqrt{s} = 8\,\mathrm{TeV}$ of pp collision data. The measurement with the di-photon channel at ATLAS is somewhat higher than that obtained with the $H \to ZZ^* \to 4\ell$ channel. However, the discrepancy is not statistically compelling and the situation is reverse with the CMS results. The ATLAS and CMS mass measurements with the two channels are combined independently (see Fig. 1). The total combined measurement yields (in GeV) [3]:

$$m_H = 125.09 \pm 0.24 = 125.09 \pm 0.21(stat.) \pm 0.11(syst.), \tag{1}$$

where the total error is split into statistical and systematics. This measurement corresponds to a stunning accuracy of 0.2%. Because of the complexity of the measurement and its sensitivity to detector performance, it is relevant to elaborate on the main sources of systematics. Figure 2 summarizes the impact of the most important groups of systematics on the mass measurement uncertainty specified above. The mass measurement result presented here is obtained by means of a likelihood ratio that includes a number of nuisance parameters. The latter incorporate the different systematic uncertainties and are profiled. As a result the nuisance parameters obtained from the fits can somewhat differ from the expected value. The total systematic error is obtained by substracting the statistical error from the total error. The most important uncertainties are instrumental and pertain to the performance of the electromagnetic calorimeters.

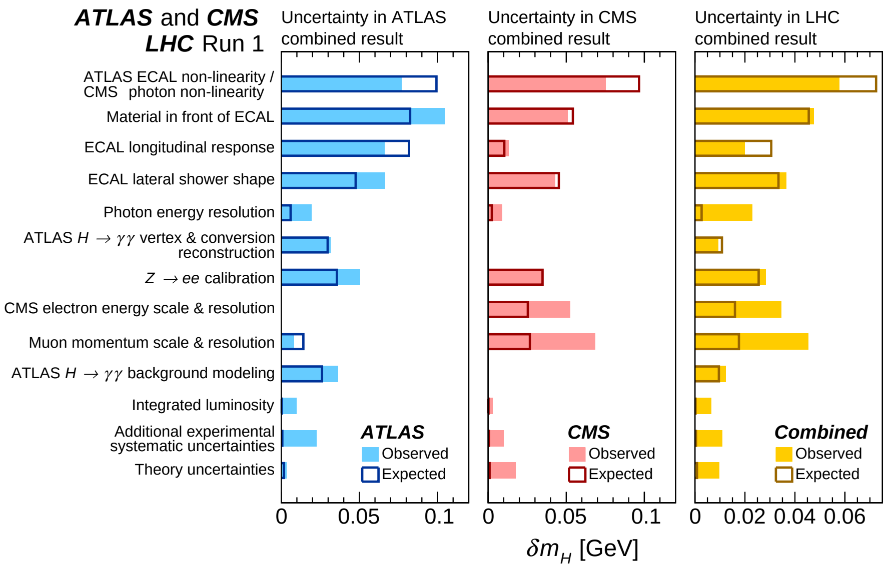

Figure 2. The impact of different groups of systematics on the ATLAS (left), CMS (center), and combined (right) mass measurement uncertainty from Ref. [3]. The observed (expected) results are shown by the solid (empty) bars (see text).

3. Spin/CP quantum numbers

The exploration of the Spin/CP quantum numbers of the newly discovered boson can be performed exploiting the properties of the decays [4] or the production mechanisms [5, 6]. These approaches are complementary. The ATLAS and CMS experiments have focused on the exploration of the decay products. This is done to understand the compability of the data with the SM hypothesis, 0^+ with respect to other hypotheses. The introduction of hypotheses other than that predicted in the SM leads to extra terms in the Lagrangian. In turn these terms generate differences in the kinematic distributions of decay products. In a recent study the ATLAS collaboration has performed a combined study of the decay kinematics of the di-photon, $H \to ZZ^* \to 4\ell$ and $H \to WW^* \to e\nu\mu\nu$ channels [7]. Here the SM is tested against two non-SM spin-0 and a simplified spin-2 hypotheses. The two non-SM spin-0 hypothesis correspond to the introduction of higher dimensional operators, including CP-conservation and CP-violation. The results exclude non-SM hypotheses considered at more than a 99% confidence level in favor of the SM. The CMS collaboration has made en extensive exploration of non-SM hypotheses with similar results in favor of the SM [8].

4. Total and differential cross-sections

The ATLAS collaboration has reported on the total and differential cross-section with the di-photon [9], the $H \to ZZ^* \to 4\ell$ [10] and their combination [11]. The results reported in Refs. [9, 10] are referred to as fiducial cross-sections. The rate of Higgs boson candidates are reported in a particular region of the phase-space defined by the decay products. Fiducial cross-sections are reported for the total phase-space explored and differentially, with respect to relevant observables (e.g. Higgs boson transverse momentum, p_T, rapidity, y, etc). Efforts are made not to bias the results with prior knowledge of Higgs boson production mechanisms in the SM. In Ref. [11] results are combined by extrapolating the fiducial cross-sections to the entire phase-space, including that where the measurement is not made and corrected by the branching fractions expected in the SM.

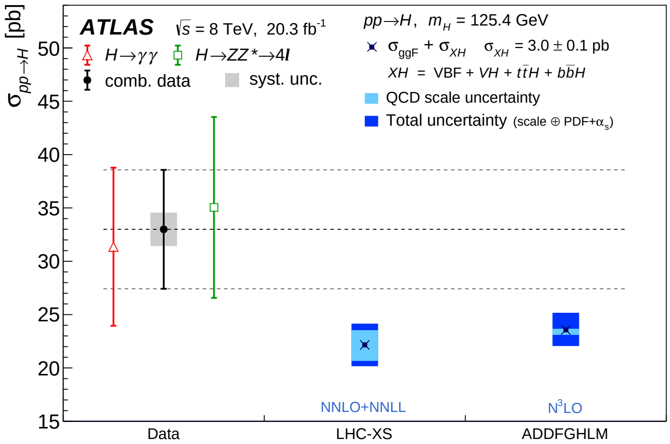

Figure 3. Measured total cross section of Higgs boson production compared to two calculations of the gluon-gluon fusion process cross section, from Ref. [11]. Contributions from other relevant Higgs boson production modes (VBF, VH, ttH, bbH) are added using cross sections and uncertainties.

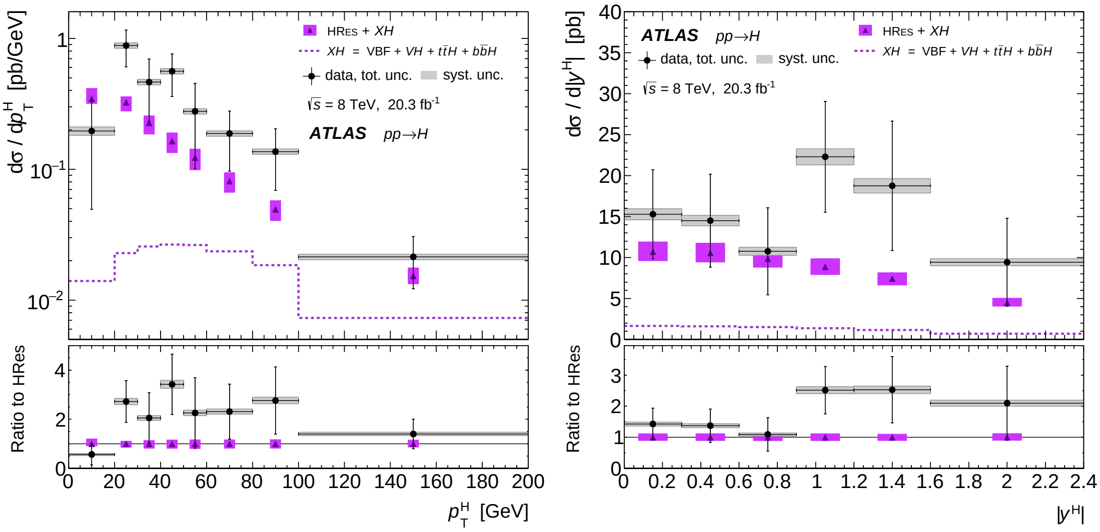

Figure 4. Differential cross-sections of the Higgs boson tranverse momentum (left) and rapidity (right) by combining the di-photon and $H \to ZZ^* \to 4\ell$ channels from Ref. [11].

Figure 3 displays the combination of the total cross-sections measured with the di-photon and the $H \to ZZ^* \to 4\ell$ channels. Results are compared to predictions existing at the time of submission to the journal. This includes an incomplete N^{3}LO cross-section for the gluon-gluon fusion production process. Since the manuscript was submitted significant progress has been made in QCD higher order corrections. The first complete gluon-gluon fusion cross-section at N^{3}LO has been made available [12]. In this calculation it is demonstrated that the correction with respect to the cross-section at NNLO evaluated at half the Higgs boson mass is about 2% and the scale uncertainty shrinks to 3%. Other production mechanisms, such as the Vector Boson Fusion, VBF, and associated production, $VH(V = Z, W)$, ttH and bbH are also taken into account.

Figure 4 displays the differential cross-sections with respect to the Higgs boson transverse

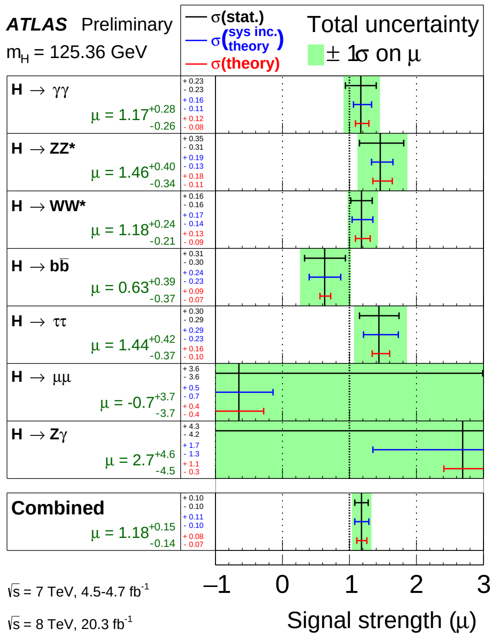

Figure 5. The observed signal strengths and uncertainties for different Higgs boson decay channels and their combination for $m_H = 125.36\,\mathrm{GeV}$. Higgs boson signals corresponding to the same decay channel are combined together for all analyses. The best-fit values are shown by the solid vertical lines. The total $\pm 1\sigma$ uncertainties are indicated by green shaded bands, with the individual contributions from the statistical uncertainty (top), the total (experimental and theoretical) systematic uncertainty (middle), and the theory systematic uncertainty (bottom) on the signal strength shown as horizontal error bars. Results are from Ref. [15].

momentum and rapidity. These results are the combination of measurements obtained with the di-photon and $H \to ZZ^* \to 4\ell$ channels. Results are compared calculations that do not include recent progress mentioned above, nor recent calculations of gluon-gluon fusion in association with one jet at NNLO [13]. These calculations signify very important progress in QCD higher order corrections that give us renewed condifence in the robustness of theoretical predictions.

In Ref. [14] it has been pointed out that the implementation of these QCD higher order corrections do not impact significantly the compatibility of the data with the SM. Other speakers in the NPR track will discuss these results from the stand point of possible physics beyond the SM. Overall, while the level of discrepancy with the SM is not strong, the study of these observables with the new data becomes very interesting.

5. Signal strength and the Standard Model

The ATLAS collaboration has recently combined results of Higgs boson yields and constraints using the $H \to \gamma\gamma, ZZ^*, WW^*, Z\gamma, b\bar{b}, \tau\tau, \mu\mu$ decays [15]. This is a global analysis in which results optimized to observe the SM Higgs boson signal are combined in a comprehensive analysis that includes variations of SM coupling strengths. The results of the individual signal strengths, or the ratio of the observed yield to that predicted by the SM and their combination are shown in Fig. 5, in terms of μ, or the observed signal yield with respect to that predicted by the SM. The combined result is [15]:

$$\mu = 1.18 \pm 0.10(stat.) \pm 0.07(syst.) \pm 0.08(theor.), \tag{2}$$

where the errors are statistical, systematics and theoretical, respectively. Strong evidence of the Vector Boson Fusion process and coupling to down-type fermions are seen with significances of $4.3\,\sigma$ and $4.5\,\sigma$, respectively. Variations of SM-like coupling strenghts lead to conclude that, overall, the data is consistent with the SM.

It is very important to note that the results discussed here are qualitatively different from those reported in section 4. Where in the latter measurements are produced without prior assumptions on production mechanisms, results reported here have predictions from the SM embedded into them. The signal strenghts are in most of the cases obtained after the application of categories. The phase-space is weighted according to how the SM Higgs boson would be produced. As a result, a certain bias towards the SM is generated.

6. Future prospects

The LHC has made strides to provide proton-proton collisions at the energy and instantaneous luminosity frontier. The first collisions at 13 TeV have been provided and recorded by the experiments. This milestone will be followed by others. Among these is the transition from 50 ns bunch spacing to 25 ns with which to reach a record instantaneous luminosity of $1.3 \times 10^{34}\,\mathrm{cm}^{-2}\mathrm{s}^{-1}$. The integrated luminosity for proton-proton collisions by the end of the year is expected to be about $10\,\mathrm{fb}^{-1}$. With the total Higgs boson cross-section expected to increase by a factor of about 2.5, comparable sensitivity will be reached with respect to that achieved in Run I. By the end of Run II, sometime in 2018, about 100-120 fb^{-1} is expected to be delivered, leading to a factor of 10 more Higgs boson candidates compared to Run I. The LHC envisions to deliver $300\,\mathrm{fb}^{-1}$ by 2023, followed by a long shutdown of about 2.5 years to pursue the high luminosity upgrade. The ultimate peak luminosity is $5.7 \times 10^{34}\,\mathrm{cm}^{-2}\mathrm{s}^{-1}$ and $4000\,\mathrm{fb}^{-1}$ of integrated luminosity by the end of the LHC's lifetime. Coupling determination may reach accuracies of 5%-10% per experiment, depending on the coupling.

7. Summary and Conclusions

Strong progress has been made by the ATLAS and CMS collaborations in determining properties of the newly discovered scalar boson. This includes the measurement of the mass with a 0.2% accuracy, the exploration of the spin/CP quantum numbers, measurement of fiducial total and differential cross-sections, and the measurement of signal strenghts, with the exploration of couplings. Run II will be critical in elucidating if physics beyond the SM is hidden in the scalar sector.

References

[1] ATLAS Collaboration (G. Aad *et al.*) 2012 *Phys.Lett.* **B716** 1
[2] CMS Collaboration (S. Chatrchyan *et al.*) 2012 *Phys.Lett.* **B716** 30
[3] ATLAS and CMS Collaborations (G. Aad *et al.*) 2015 Phys. Rev. Lett. **114** 191803
[4] Dell Aquila J R and Nelson C A 1986 Phys. Rev. **D33** 80
[5] Englert C, Goncalves-Netto D, Mawatari K and Plehn T 2013 JHEP **1301** 148
[6] Djouadi A, Godbole R, Mellado B and Mohan K 2013 Phys. Lett. **B723** 307
[7] ATLAS Collaboration (G. Aad *et al.*) 2015 ATLAS-CONF-2015-008
[8] CMS Collaboration (V. Khachatryan *et al.*) 2014 arXiv:1411.3441 [hep-ex]
[9] ATLAS Collaboration (G. Aad *et al.*) 2014 JHEP **1409** 112
[10] ATLAS Collaboration (G. Aad *et al.*) 2014 Phys. Lett. B **738** 234
[11] ATLAS Collaboration (G. Aad *et al.*) 2015 Phys.Rev.Lett. **115** no.9, 091801
[12] Anastasiou C, Duhr C, Dulat F, Herzog F and B. Mistlberger 2015 Phys. Rev. Lett. **114** no. 21 212001
[13] Boughezal R, Caola F, Melnikov K, Petriello F and Schulze M (2015) arXiv:1504.07922 [hep-ph]
[14] von Buddenbrock S, Chakrabarty N, Cornell A S, Kar D, Kumar M, Mandal T, Mellado B, Mukhopadhyaya B and Reed R (2015) arXiv:1506.00612 [hep-ph]
[15] ATLAS Collaboration (G. Aad *et al.*) 2015 ATLAS-CONF-2015-007